*Journal of Ceramic Processing Research. Vol. 22, No. 3, pp. 289~295 (2021)*
*(Received 18 May 2020, Received in revised form 2 July 2020, Accepted 16 July 2020)*
*https://doi.org/10.36410/jcpr.2021.22.3.289*

J O U R N A L O F
**Ceramic Processing Research**

# Effects of pressureless two-step sintering on the densification and properties of tetragonal zirconia

**H.C. Alexander Chee[a], R.S.K. Singh[a,b] and K.Y. Sara Lee[c,*]**
[a]*Faculty of Engineering, University of Malaya, 50603 Kuala Lumpur, Malaysia*
[b]*Faculty of Engineering, Universiti Teknologi Brunei, Tungku Highway, Gadong BE1410, Brunei Darussalam*
[c]*Tunku Abdul Rahman University College, Faculty of Engineering & Technology, Department of Mechanical Engineering, 53300, Kuala Lumpur, Malaysia*

**The effects of pressureless two-step sintering (TSS) on the densification and mechanical properties of tetragonal zirconia polycrystals were investigated and compared with that obtained by conventional single-step sintering (SSS). The TSS profile involved firing at a high temperature, $T_1$ of 1450 ºC followed by cooling to a lower temperature, $T_2$ of 1250 ºC and soaking for various holding time ranging from 2 h to 10 h. The results showed that the tetragonal phase stability was not disrupted by TSS. A high relative density, above 96%, was obtained for the TSS samples regardless of holding time when compared to SSS which exhibited about 99% of theoretical density when sintered at 1450 ºC. Nonetheless, the beneficial effects of TSS in enhancing the Vickers hardness and fracture toughness of tetragonal zirconia when compared to SSS, without incurring grain growth have been revealed. The single-step sintering yielded large tetragonal grains, about 0.56 μm, if compared TSS which exhibited a refine microstructure having grain sizes ranging from 0.27 μm (for 2 h holding time) to 0.35 μm (for 10 h holding time). This feature of TSS which allows for the inhibition of grain boundary migration and the activation of grain boundary diffusion at lower dwelling temperature during sintering were responsible for the enhancement of the mechanical properties of tetragonal zirconia.**

**Key words: two-step sintering (TSS), single-step sintering (SSS), mechanical properties, zirconia, Y-TZP.**

## Introduction

Tetragonal zirconia polycrystals is an interesting ceramic for a variety of applications because of its chemical inertness, superior wear and mechanical properties when compared to other monolithic ceramics [1-3]. Typically, zirconia-based ceramics have been used in many engineering applications including as high-performance thermal barrier coatings for aero-engines [4], electrolyte material for solid oxide fuel cells [5], gas and electrochemical sensor devices [6, 7] and catalysts support [8]. In addition, the excellent biocompatibility and its natural tooth-like colour of tetragonal zirconia have also widened its application as implants in dental restorations [9-11] as well as bone cement and hip joint prosthesis [12-14]. In recent years, there has been arouse interest and success in using additive manufacturing technologies in the fabrication of complex-shaped zirconia components and it is envisaged that this would open up new avenues in other fields for the use of zirconia [15].

Pure zirconia is known to exist in three different allotropes: the monoclinic phase exists from room temperature up to ~1170 ºC, the tetragonal form (1170 ºC to ~2370 ºC), and the cubic symmetry (2370 ºC to ~2680 ºC) [16]. However, the retention of a fully tetragonal matrix at room temperature is made possible when pure zirconia is stabilised by blending with 2-3 mol% of yttria, and this ceramic exhibits the best mechanical properties at room temperature [17-21].

The properties of the tetragonal zirconia would depend very much on the ceramic processing techniques which determine the properties of the starting powder (e.g. nano-sized versus micron-sized) and thereafter the consolidation method used to form a useful solid body [22-26]. Typically, tetragonal zirconia can be densified using conventional single-step sintering (SSS) method and/or non-conventional sintering techniques such as hot pressing [27], microwave sintering [28], spark plasma sintering [29], rapid sintering [30], cold sintering [31], hot-isostatic pressing [32], pulsed electric current sintering [33], etc. In most literatures, these non-conventional sintering methods have been reported to be viable in aiding densification when compared to conventional sintering, resulting in fine grained microstructure and improved mechanical properties. This enhancement however comes with several limitations including re-strictions in the fabrication of samples having intricate shape and size, upscaling for mass production, ease of

*Corresponding author:
Tel : +(6)03-41450123
Fax: +(6)03-41423166
E-mail: leeky@tarc.edu.my

accessibility to the equipment, and the high cost associated with the complexity of the systems or equipment needed in the consolidation process.

Sintering is an important process in the fabrication of tetragonal zirconia artefacts through the application of heat at a temperature below the melting point of the ceramics. During this process, densification takes place as a result of the reduction in the surface area of the co-joining particles. The objective is to facilitate particles consolidation through a complex diffusion and mass transfer mechanisms which occur concurrently at the surface, bulk and grain boundaries [34]. However, in order to achieve high densities, typical conventional SSS approach often requires the use of high sintering temperatures and long holding times which often resulted in accelerated grain growth which occurs in the final stage of sintering [35]. In addition, the formation of some cubic phase is inevitable when sintered at high temperatures and this has an adverse effect on the durability of the sintered body [19, 36]. This has posed a challenge and many researchers have examined the effects of two-step sintering (TSS) as an alternative low-cost sintering method. Chen and Wang [37] were amongst the pioneer to demonstrate the viability of TSS in promoting densification via grain boundary diffusion in yttrium oxide and restraining grain boundary migration thus avoiding grain coarsening.

In TSS, the ceramic is heated to a temperature, $T_1$, hold for a short time and then rapidly cooled to a lower temperature, $T_2$, hold at this temperature for a pre-determined time for densification to proceed without inducing grain growth, before cooling down to room temperature. Because of its simplicity in the implementation, various ceramics have been sintered via TSS including Ce-TZP [38, 39], $Al_2O_3$ [40], $SnO_2$ [41], tungsten [42], lead-free $(K_{0.5}Na_{0.5})NbO_3$ piezoelectric ceramics [43] and other ceramics [44]. In all these studies, the effectiveness of the TSS, however were found to be dependent on the starting powder properties as well as the sintering parameters adopted. For instance, Mazaheri et al. [45] reported that a proper TSS regime would be required to achieve the goal of enhancing densification without inducing grain growth. They varied the TSS profile and evaluated the densification behaviour of nanocrystalline ZnO. The results indicated that regardless of holding time, there was a critical temperature for $T_2$, below which resulted in grain growth without any improvement in densification.

In another related study, the authors [46] studied the sintering behavior of 8 mol% yttria-stabilised zirconia by performing TSS at $T_1$ = 1250 ºC and $T_2$ = 1050 ºC. They observed a significant enhancement in the relative density, from about 82 % to about 98 %, as the holding time at $T_2$ increased from 0 to 20 h, respectively. This enhancement in densification was not accompanied by grain growth as the grain sizes remained almost the same, at about 250 nm, regardless of the holding time. Zhang et al. [38] studied the effects of different TSS conditions on the densification and properties of 12Ce-TZP. They found that the optimum sintering regime of $T_1$ = 1400 ºC/1 min. hold, $T_2$ = 1300 ºC/30 h were required to achieve high density at a lower grain growth rate as well as optimized mechanical properties.

In this work, the sintering behaviour and mechanical properties of tetragonal zirconia stabilised with 3 mol% yttria prepared by pressureless TSS were investigated and compared with that produced by SSS.

## Experimental

In the present work, a commercial 3 mol% Y-TZP powder (Kyoritsu Corp., Japan) was used as the starting ceramics without further processing. In a typical sample preparation, about 3 g of powders were weigh using an electronic balance and placed in a metal mold having diameter of 20 mm. The samples were uniaxially pressed at about 80 MPa to form disc sample. After that the compacts were subjected to cold-isostatic pressing at 200 MPa to obtained the green samples [19]. The pressureless sintering in this work was carried out in a rapid-heating box furnace, comparing two-step sintering (TSS) with conventional single-step sintering (SSS) cycle. The TSS was carried out as follows: in the first stage the samples were heated at a ramp rate of 10 ºC/min. to $T_1$ = 1450 ºC and held for 1 min. The samples were then cooled at a cooling rate of 10 ºC/min. to a lower temperature of $T_2$ = 1250 ºC and held for varying holding times (2 h, 4 h, 6 h, 8 h and 10 h) before cooling naturally in the furnace to room temperature. In contrast, the SSS was performed at the final temperature, $T$ of 1250 ºC and 1450 ºC, with a heating rate of 10 ºC/min. and held for 2 h before allowing to cool in the furnace to room temperature. The sintering regimes used in this work are shown in Fig. 1. However, in order to demonstrate the influence of conventional single-step sintering on the tetragonal grain size and relative density, additional samples were prepared and

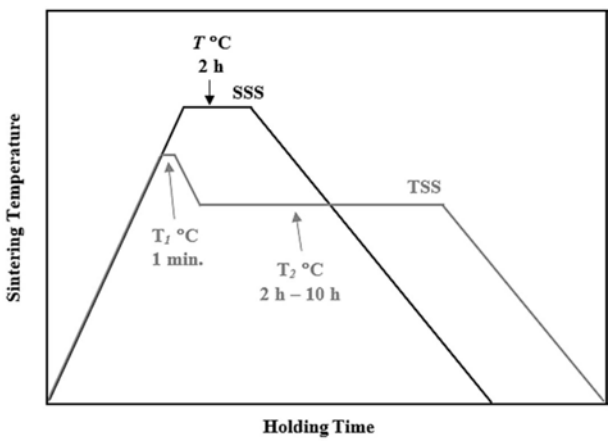


**Fig. 1.** A schematic diagram showing the TSS and conventional SSS schemes used in the present work.

pressureless sintered at other temperatures between 1100 °C and 1500 °C.

The water immersion method based on Archimedes principle was used to obtain the bulk density of sintered samples using a Mettler Toledo Balance AG204 densimeter, with deionised water as the medium. For this purpose, the weight of the sample was first taken in air and then when submerged in water. The test condition was in accordance to ISO18754 [47]. The bulk density was determined and the relative density was calculated by taking the theoretical density for tetragonal zirconia as 6.09 g/cm$^3$ [48]. All the sintered samples were ground successively on one face by SiC papers of varying grades, from 120 (rough) to 1200 (fine), followed by final polishing using diamond paste (6 μm and 1 μm) to obtain an optical reflective surface. Vickers Hardness ($H_v$) was measured on polished samples using the Vickers indentation method in accordance to a standard test method, using the equation given in Eq. (1) [49]. The indention load was kept constant at 10 kgf with loading time of 10 s.

$$H_v = 0.4635 P/a^2 \tag{1}$$

where, $P$ is the indentation load and $a$ is the indent half diagonal.

The fracture toughness ($K_{Ic}$) of the sintered body was obtained from the geometry parameters of the Vickers indent using the relationship derived by Niihara et al. [50] as given in Eq. (2). The average values for $H_v$ and $K_{Ic}$ were taken from six measurements made for each sample.

$$K_{IC} = 0.035\left(\frac{a}{l}\right)^{0.5}\left(\frac{E\beta}{H_v}\right)^{0.4}\left(\frac{H_v}{\beta}\right)a^{0.5} \tag{2}$$

where, $l$ is the average crack length, $E$ is the Young's Modulus, $H_v$ is the Vickers hardness and $\beta$ is the constraint factor which was taken as 3 for tough ceramics such as tetragonal zirconia [51].

Microstructural evolution of the sintered samples was examined by using the scanning electron microscope (SEM). Prior to SEM analysis, the samples were thermal etched at a temperature 50 °C below the sintering temperature and held for 30 min. before cooling to room temperature. The average grain size of the samples was determined from the SEM micrographs by using the line intercept method [52]. X-ray diffraction (XRD) was used to examine the phase present, taken over the $2\theta$ of 27° to 33° which covers the monoclinic ($m$) and tetragonal ($t$) dominant (111) peaks, with 0.02° step size using Cu-Kα radiation operating at 45 kV and 40 mA. The peaks corresponding to the characteristics of $t$-$ZrO_2$ and $m$-$ZrO_2$ were identified using JCPDS files no. 48-0224 and 37-1484, respectively. The monoclinic and tetragonal phase content were calculated using the relationship proposed by Toraya et al. [53]:

$$X_m = \frac{I(111)_m + I(11\bar{1})_m}{I(111)_m + I(11\bar{1})_m + I(111)_t} \tag{3}$$

$$V_m = \frac{1.311 X_m}{1 + 0.311 X_m} \times 100\% \tag{4}$$

$$V_t = 100\% - V_m\,\% \tag{5}$$

where $X_m$ is the integrated intensity ratio, $I(111)_m$ and $I(111)_t$ are the peak intensity of the monoclinic and tetragonal phase, respectively, $V_m$ and $V_t$ are the calculated volume fraction of the monoclinic and tetragonal phase, respectively.

## Results and Discussion

The phase analysis by XRD of the sintered samples as shown in Fig. 2, revealed a fully tetragonal structure exists regardless of sintering profile. The fact that no monclininc phase was detected after the TSS sintering, this indicates that the prolong holding time, up to 10 h, have little effect on the stabilization of the tetragonal structure. This was also verified by Rietveld anlaysis which showed that the tetrgonality i..e. $c/a$ lattice parameter ratio of the tetrgonal zirconia did not

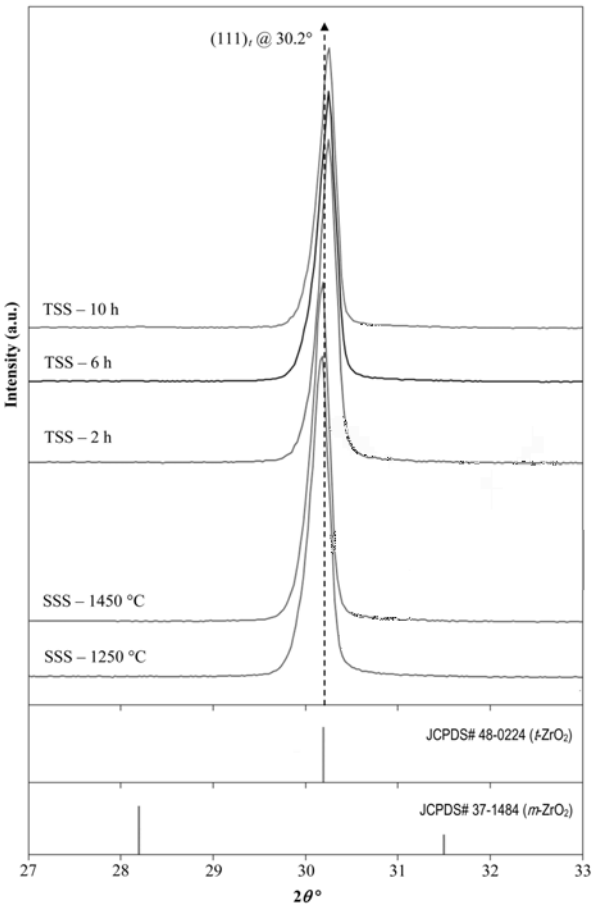


**Fig. 2.** XRD analysis of the samples prepared by SSS and TSS revealing the presence of a tetragonal structure.

changed very much after sintering; for example the *c/a* ratio of the 10 h holding time sample was 1.4292 as compared to 1.4312 based on the tetragonal standard (JCPDS no. 48-0224). This observation was also in good agreement with the findings of other researchers [38, 46]. Nevertheless, the $(111)_t$ tetragonal peak of the TSS samples was found to have shifted slightly towards higher angles, by about 0.15°. This small peak shift in the fractions of an angle can be attributed to lattice strain resulting from prolong sintering during TSS rather than crystallographic phase change in the zirconia matrix [54].

The effects of TSS and SSS on the relative density of tetragonal zirconia are shown in Fig. 3. As expected in the SSS profile, the relative density increased with increasing sintering temperature i.e. from 95.9% at 1250 C to > 99% at 1450 °C, but was accompanied by significant grain growth. In the case of TSS profile, the relative density of the sample sintered for 2 h showed an improvement if compared to the SSS-1250 C sample. Further increased in the TSS holding time from 2 h to 10 h, was followed by a steady increase in the relative density, i.e. from 96.5% to about 98.5%, respectively but with no significant grain growth.

In the conventional SSS scheme, the size of the tetragonal grains was found to increased at a slower rate as the temperature risen from 1100 °C to 1300 °C. However during this period, densification proceeded rapidly with increasing temperature as depicted by the inset graph in Fig. 4. However, as the sintering temperature increased beyond 1300 °C, there was a marginal enhancement in density, but the rate of grain growth, resulting from grain boundary migration, was rapid. This is evident from Fig. 4 where the average tetragonal grains continued to grow from about 0.4 µm to 0.6 µm when sintered at 1500 °C. A similar densification trend for 3 mol% Y-TZP was reported by Suárez et al. [55]. The authors found that the onset of densification started at about 1100 °C and the relative density increased with increasing sintering temperature, subsequently reached a plateau of about 99% when sintered at 1400 °C as compared to 1350 °C observed in the present work.

In contrast, the TSS was found to be effective in suppressing grain growth at the final stage of sintering as shown in Fig. 5, while allowing densification to proceed as can be seen in Fig. 3. It can be noted that as the holding time increased from 2 h to 10 h, this was accompanied by a small increase in the grain sizes, from 0.27 µm to 0.35 µm, respectively although the relative density was higher than 96%. The SEM micro-structures of the sintered samples comparing the TSS and SSS samples sintered at 1250 °C are shown in Fig. 6. In general, regardless of the sintering regime, an equiaxed grain structure was observed which is typically a dense tetragonal zirconia having above 95% of theoretical density [56]. The main difference between

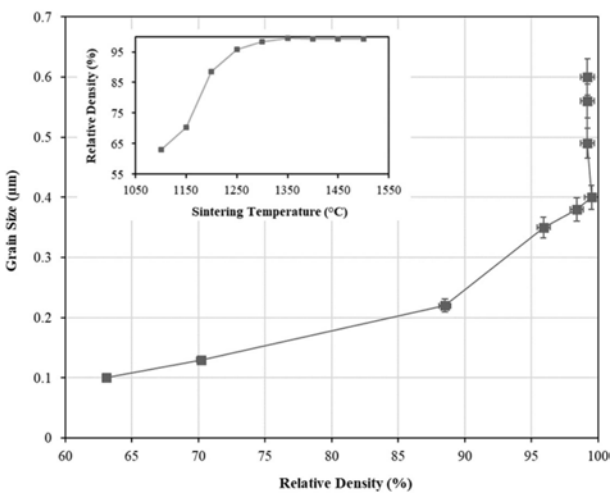


**Fig. 4.** The tetragonal grain size as a function of relative density of samples subjected to conventional single-step sintering from 1100 °C to 1500 °C. The inset shows the variation in relative density with sintering temperature.

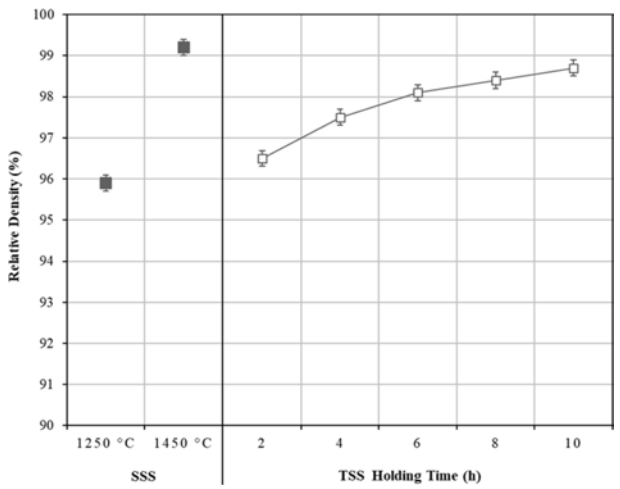


**Fig. 3.** The effects of SSS and TSS on the densification of tetragonal zirconia.

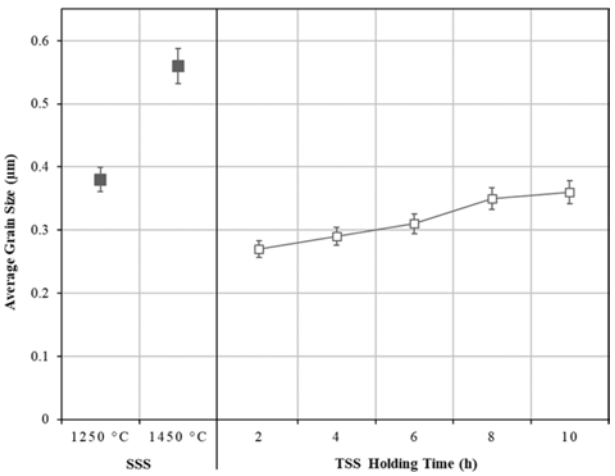


**Fig. 5.** The effects of SSS and TSS on the tetragonal grain size of zirconia.

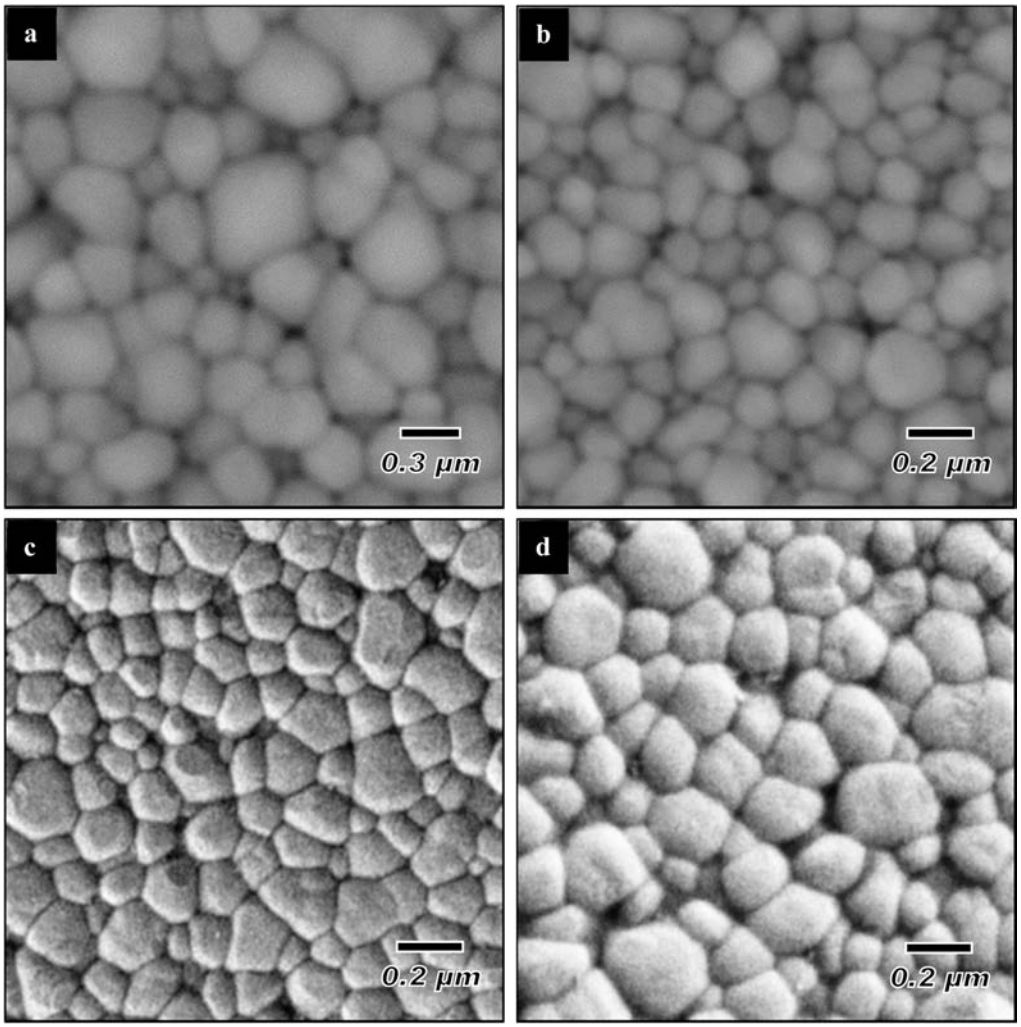


**Fig. 6.** Typical SEM microstructure of (a) SSS-1250 ºC and TSS samples at varying holding times: (b) 2 h, (c) 4 h and (d) 10 h [59].

the microstructures would be their average grain size as depicted in Fig. 5.

In another study, Suárez et al. [57] observed a similar microstructural development in their Y-TZP with TSS exhibiting finer tetragonal grain size. Mazaheri et al. [58] reported that there exists an incubation period for grain growth during TSS. They observed significant grain growth when the holding time exceeded 20 h. A fully dense structure would only be possible with appreciable grain growth, although the final grain size may still be smaller than that of SSS [59].

The effects of TSS on the mechanical properties of tetragonal zirconia are shown in Fig. 7. In general, the Vickers hardness and fracture toughness were improved when subjected to TSS. The average Vickers hardness and fracture toughness were observed to increase monotonically, from 12.9 GPa to 13.7 GPa and 7.8 $MPam^{1/2}$ to 8.2 $MPam^{1/2}$, respectively with increasing holding time. This improvement in the mechanical properties was attributed to the active grain boundary diffusion during two-step sintering which resulted in porosity diminution and the formation of a network of

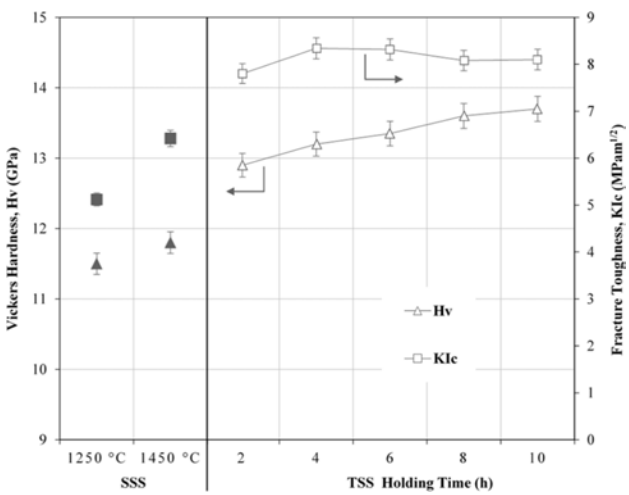


**Fig. 7.** The effects of SSS and TSS on the Vickers hardness and fracture toughness of tetragonal zirconia.

finer tetragonal grains.

These findings agreed with the observation reported by Mazehari et al. [46] for 8 mol% YSZ. More specifi-

cally, the authors found that fracture toughness of the zirconia increased by twofold when subjected to TSS. A similar observation was also reported for other ceramics subjected to two-step sintering. Li et al. [42] compared the sintering behaviour of tungsten subjected to conventional sintering at temperatures ranging from 1100 C to 1600 ºC and soaking times up to 3 h versus TSS at $T_1$ ranging from 1300 ºC to 1450 ºC and holding of 1 h, and $T_2$ ranging from 1200 ºC to 1350 ºC and holding for 10 h. They found that high densities of above 98% of theoretical could only be achieved by normal sintering above 1500 ºC/3h holding time with extensive grain growth. In contrast, regardless of the TSS profile used, the tungsten could achieve similar densification as the conventional sintering but without abnormal grain growth. In fact, the grain sizes of the TSS samples were reduced by more than 50% than that obtained by conventional sintering and this was accompanied by a significant improvement in the bending strength, hardness and Young's modulus. This trend of improvement is similar as that observed in the present work. In addition, Li et al. found that the mechanical reliability of the TSS samples was also improved, i.e. the Weibull modulus of the TSS samples was $m$ = 42 compared to $m$ = 24 for the conventional sintered samples. More recently, Lóh et al. [40] demonstrated the effectiveness of TSS in the consolidation of alumina ceramics. The authors concluded that the $T_2$ has a significant effect on the final density whereas the combination of $T_2$ and holding time would influence the final grain size of the sintered body.

## Conclusions

The present work demonstrated the effectiveness of two-step sintering in promoting densification of tetragonal zirconia without incurring significant grain growth as typically observed for conventional single-step sintering. It was revealed that a relative density of above 97% could be attained without undergoing excessive grain growth as observed for the conventional single-step sintered samples. The tetragonal grain sizes of the TSS samples varied between 0.27 μm to about 0.35 μm, depending on the holding time and these values were about 40-50% lower than that obtained by SSS. In addition, the mechanical properties of the TSS zirconia were greatly improved when compared to the SSS zirconia and this was attributed to the finer tetragonal microstructure achieved through the two-step sintering scheme.

## References

1. T. Masaki, J. Am. Ceram. Soc. 69[8] (1986) 638-640.
2. Z. Xiao, S. Yu, Y. Li, S. Ruan, L.B. Kong, Q. Huang, Z. Huang, K. Zhou, H. Su, Z. Yao, W. Que, Y. Liu, T. Zhang, J. Wang, P. Liu, D. Shen, M. Alli, J. Zhang, and D. Tang, Mater. Sci. Eng. R 139 (2020) 100518.
3. T.A. Otitoju, P.U. Okoye, G. Chen, Y. Li, M.O. Okoye, and S. Li, J. Ind. Eng. Chem. 85 (2020) 34-65.
4. Q. Liu, S. Huang, and A. He, J. Mater. Sci. Technol. 35[12] (2019) 2814-2823.
5. S.-J. Hao, C. Wang, T.-L. Liu, Z.-M. Mao, Z.-Q. Mao, and J.-L. Wang, Int. J. Hydrogen Energy 42[50] (2017) 29949-29959.
6. J. Wang, L. Zhao, J. Li, F. Liu, R. You, S. Lv, Z. Yang, J. He, Y. Hao, X. Yan, C. Wang, X. Liang, P. Sun, and G. Lu, Sens. Actuators, B 316 (2020) 128199.
7. T. Liu, X.F. Zhang, L. Yuan, and J. Yu, Solid State Ionics 283 (2015) 91-102.
8. G.X. Yan, A. Wang, I.E. Wachs, and J. Baltrusaitis, Appl. Catal., A 572 (2019) 210-225.
9. J. Grech and E. Antunes, J. Mater. Res. Technol. 8[5] (2019) 4956-4964.
10. H. Nishihara, M.H. Adanez, W. Att, J. Prosthodontic Res. 63[1] (2019) 1-14.
11. K. Sivaraman, A. Chopra, A.I. Narayan, and D. Balakrishnan, J. Prosthodontic Res. 62[2] (2018) 121-133.
12. J. Chevalier, and L. Gremillard, Compr. Biomater. II 1 (2017) 122-144.
13. I. Denry, and J.A. Holloway, Materials 3[1] (2010) 351-368.
14. N.A. Patil and B. Kandasubramanian, Ceram. Int. 46[4] (2020) 4041-4057.
15. X. Zhang, X. Wu, and J. Shi, J. Mater. Res. Technol. 9[4] (2020) 9029-9048.
16. R.C. Garvie, R.H. Hannink, and R.T. Pascoe, Nature 258[5537] (1975) 703-704.
17. Y. Xu, Z. Huang, Y.G. Liu, M. Fang, L. Yin, and M. Guan, Solid State Sci. 14[6] (2012) 730-734.
18. M. Xue, S. Liu, X. Wang, and K. Jiang, Mater. Chem. Phys. 244 (2020) 122693.
19. R. Singh, C. Gill, S. Lawson, and G.P. Dransfield, J. Mater. Sci. 31[22] (1996) 6055-6062.
20. S. Ramesh, C. Gill, and S. Lawson, J. Mater. Sci. 34[22] (1999) 5457-5467.
21. S. Ramesh, K.Y. Sara Lee, and C.Y. Tan, Ceram. Int. 44[17] (2018) 20620-20634.
22. M. Lakusta, I. Danilenko, G. Volkova, L. Loladze, G. Golovan, I. Brukhanova, V. Glazunova, I. Popov, O. Mazur, and T. Konstantinova, Ceram. Int. 46[9] (2020) 13953-13960.
23. D.R.R. Lazar, M.C. Bottino, M. Özcan, L.F. Valandrod, R. Amaral, V. Ussui, and A.H.A. Bressiani, Dental Mater. 24[12] (2008) 1676-1685.
24. A.H. Nur Nadia, S. Ramesh, C.Y. Tan, Y.H. Wong, N.I. Zainal Abidin, W.D. Teng, U. Sutharsini and Ahmed A.D. Sarhan, J. Ceram. Process. Res. 18[7] (2017) 483-487.
25. C.H. Ting, S. Ramesh, C.Y. Tan, N.I. Zainal Abidin, W.D. Teng, I. Urries, and L.T. Bang, J. Ceram. Process. Res. 18[8] (2017) 569-574.
26. C.K. Ng, S. Ramesh, C.Y. Tan, C.Y. Ching, N. Lwin, and A. Muchtar, J. Ceram. Process. Res. 17[5] (2016) 443-447.
27. G. Bernard-Granger, N. Monchalin, and C. Guizard, Mater. Letts. 62[30] (2008) 4555-4558.
28. S. Ramesh, N. Zulkifli, C.Y. Tan, Y.H. Wong, F. Tarlochan, S. Ramesh, W.D. Teng, I. Sopyan, L.T. Bang, and A.A.D. Sarhan, Ceram. Int. 44[8] (2018) 8922-8927.
29. W. Li and L. Gao, J. Eur. Ceram. Soc. 20[14-15] (2000) 2441-2445.
30. V. Prajzler, S. Průša, and K. Maca, J. Eur. Ceram. Soc. 39[16] (2019) 5309-5319.

31. H. Guo, T.J.M. Bayer, J. Guo, A. Baker, and C.A. Randall, Scr. Mater. 136 (2017) 141-148.
32. A. Dash, B.-N. Kim, J. Klimke, and J. Vleugels, J. Eur. Ceram. Soc. 39[4] (2019) 1428-1435.
33. R. Muccillo and E.N.S. Muccillo, J. Eur. Ceram. Soc. 34[15] (2014) 3871-3877.
34. J.E. Blendell, in "Encyclopedia of Materials: Science and Technology, 2nd Edition" (Pergamon, 2001) p. 8745-8750.
35. C.P. Cameron and R. Raj, J. Am. Ceram. Soc. 71[12] (1988) 1031-1035.
36. J. Chevalier, S. Deville, E.Munch, R. Jullian, and F. Lair, Biomater. 25[24] (2004) 5539-5545.
37. I.W. Chen, and X.H. Wang, Nature 404[6774] (2000) 168-171.
38. W. Zhang, J. Bao, G. Jia, W. Guo, X. Song, and S. An, J. Alloys Compd. 711 (2017) 686-692.
39. S. Bejugama, N.K. Gadwal, and A.K. Pandey, Ceram. Int. 45[8] (2019) 10348-10355.
40. N.J. Lóh, L. Simão, J. Jiusti, S. Arcaro, F. Raupp-Pereira, A. De Noni Jr., and O.R.K. Montedo, Ceram. Int. 46[8] (2020) 12740-12743.
41. M.M. Shahraki, M.D. Chermahini, S. Alipour, P. Mahmoudi, I. Safaee, and M. Abdollahi, J. Alloys Compd. 805 (2019) 794-801.
42. X. Li, L. Zhang, Y. Dong, R. Gao, M. Qin, X. Qu, and J. Li, Acta Mater. 186 (2020) 116-123.
43. G. Ye, J. Wade-Zhu, J. Zou, T. Zhang, T.W. Button, and J. Binner, J. Eur. Ceram. Soc. 40[8] (2020) 2977-2988
44. N.J. Lóh, L. Simão, C.A. Faller, A. DeNoni Jr., and O.R.K. Montedo, Ceram. Int. 42[11] (2016) 12556-12572.
45. M. Mazaheri, A.M. Zahedi, and S.K. Sadrnezhaad, J. Am. Ceram. Soc. 91[1] (2008) 56-63.
46. M. Mazaheri, M. Valefi, Z.R. Hesabi, and S.K. Sadrnezhaad, Ceram. Int. 35[1] (2009) 13-20.
47. ISO, No.18754:2020 (2020) p.1-10.
48. T. K. Gupta, F. F. Lange and J. H. Bechtold , J. Mater. Sci. 13[7] (1978) 1464-1470.
49. ISO, No.14705:2016 (2016) p.1-20.
50. K. Niihara, R. Morena, and D.P.H. Hasselman, J. Mater. Sci. Lett. 1[1] (1982) 13-16.
51. A.G. Evans and E.A. Charles, J. Am. Ceram. Soc. 59[7-8] (1976) 371-372.
52. M.I. Mendelson, J. Am. Ceram. Soc. 52[8] (1969) 443-446.
53. H. Toraya, M. Yoshimura, and S. Sōmiya, J. Am. Ceram. Soc. 67[9] (1984) C-183-C-184.
54. N.A.-H. Husain, J. Camilleri, and M. Özcan, J. Mech. Behav. Biomed. Mater. 64 (2016) 104-112.
55. G. Suárez, Y. Sakka, T.S. Suzuki, T. Uchikoshi, and E.F. Aglietti, J. Ceram. Soc. Jpn. 117[1364] (2009) 470–474.
56. U. Sutharsini, M. Thanihaichelvan, C.H. Ting, S. Ramesh, C.Y. Tan, Hari Chandran, A.A.D. Sarhan, S. Ramesh, and I. Urriés. Ceram. Int. 43[10] (2017) 7594-7599.
57. G. Suárez, Y. Sakka, T.S. Suzuki, T. Uchikoshi, X. Zhu, and E.F. Aglietti, Sci. Technol. Adv. Mater. 10[2] (2009) 025004.
58. M. Mazaheri, A. Simchi, and F. Golestani-Fard, J. Eur. Ceram. Soc. 28[15] (2008) 2933-2939.
59. S. Ubenthiran, in "The Effect of Sintering Parameters on The Mechanical Properties and Hydrothermal Ageing Resistance of Y-TZP Ceramic" (University of Malaya, 2015) p.73-117.